The EMBO Journal vol.13 no.4 pp.751 – 757, 1994

Origins of reversed directionality in the ncd molecular motor

A.Lockhart and R.A.Cross[1]

Molecular Motors Group, Marie Curie Research Institute, Oxted RH8 0TL, Surrey, UK
[1]Corresponding author

Communicated by J.V.Small

The head or motor domain of the ncd (non-claret disjunctional) molecular motor is 41% identical to that of kinesin, yet moves along microtubules in the opposite direction to kinesin. We show here that despite the reversed directionality of ncd, its kinetics in solution are homologous in key respects to those of kinesin. The rate limiting step, ADP release, occurs at 0.0033 s^{-1} at 100 mM NaCl and is accelerated ~1000-fold when the motor binds to microtubules. Other reaction steps are all very fast (>0.1 s^{-1}) compared with ADP release, and the motor is consequently paused in the ncd.ADP state until microtubule binding occurs (K_d = 2 μM), at which point ADP release is triggered and the motor locks onto the microtubule in a rigor-like state. These data identify close functional homology between the strong binding states of kinesin and ncd, and in view of this we discuss a possible mechanism for directional reversal, in which the strong binding states of ncd and kinesin are functionally identical, but the weak binding states are biased in opposite directions.

Key words: molecular motors/kinesin/mechanochemical coupling/microtubule motor/ncd

Introduction

Non-claret disjunctional (ncd) is a molecular motor which moves towards the minus ends of microtubules. The protein is a member of the kinesin superfamily of proteins (Endow, 1991; Goldstein, 1991). Mutant *Drosophila* lacking the ncd motor have defective chromosome disjunction (Endow *et al.*, 1990), due to incorrect spindle assembly and spindle pole formation (Hatsumi and Endow, 1992). The ncd molecule comprises twin N-terminal domains, believed to be responsible for cargo binding, and twin C-terminal motor domains, separated by a stalk region of predicted coiled-coil (Chandra *et al.*, 1993). The motor domains contain the ATPase and microtubule binding functions of the molecule. This modular arrangement is typical of the superfamily (Vale and Goldstein, 1990), although the ordering of the modules differs amongst the members, so that for example in kinesin itself, the motor domain is N-terminal and the cargo binding domain is C-terminal (Scholey *et al.*, 1989). Within the motor domain, ncd and kinesin are 41% identical in amino acid sequence, so the discovery that ncd is minus-end directed (McDonald *et al.*, 1990; Walker *et al.*, 1990) immediately raised the intriguing question of how two such structurally similar motors might move in opposite directions. The direction of sliding is an intrinsic property of the motor domain (Stewart *et al.*, 1993), so it is clear that analysis of the structural and/or kinetic differences between these two oppositely directed motors should reveal the determinants of directionality.

Molecular motors generate force via their power stroke, a force generating transition between two attached conformations of the motor. Reversing the direction of motility requires that the power stroke exert force in the opposite direction. The structural details of the power stroke are not yet understood for any motor, but the biochemical coupling of ATP turnover to force generation is relatively well-characterized, at least for myosin and kinesin. In general, force production is coupled to ATP turnover because at least one of the biochemical steps of ATP turnover is powerfully accelerated (typically 1000-fold) by the binding of the motor to its track (Hackney, 1992). The effect of this is to pause the motor at the coupled kinetic step until it binds to its track, at which point the coupled step is accelerated and its associated power stroke can occur. For myosin, the best characterized motor, force generation is coupled to product release. Binding of the myosin motor to an actin filament triggers the release of product γ-phosphate (P_i) and ADP (Geeves, 1989), locking the motor onto the actin filament and generating force. Rebinding of ATP returns the motor to its relatively weakly bound starting state. For kinesin, the coupling appears similar, with the ADP-release step rate-limiting and accelerated by microtubule binding (Hackney, 1992), albeit force may be produced in a subsequent transition, rather than at the coupled step itself (Romberg and Vale, 1993).

Figure 1 illustrates the two principal ways in which the power stroke of a minimal (two-state) motor might be reversed. In the conventional scheme in Figure 1a, the motor drives from conformational state 1 into state 2, exerting force. Reversal of the power stroke might most simply be achieved as shown in Figure 1b. The motor still drives from state 1 into state 2, but force is produced in the opposite direction because of a structural *volte-face* within the motor–track complex (shown here at the track–motor interface). Alternatively, and less obviously, reversal could be achieved as shown in Figure 1c, by preserving the structures of states 1 and 2, but adjusting the coupling such that ATP turnover drives the motor from state 2 into state 1, equivalent to driving the conventional power stroke backwards. This possibility was recently discussed by Taylor (1993). Here, we report that despite its reversed directionality relative to kinesin, ncd has very similar ATPase kinetics to kinesin, and an identical mode of coupling to microtubule binding. Given these data, we argue that it is highly unlikely that ncd is coupled backwards relative to kinesin. Rather, the kinetic homology between ncd and kinesin leads us to favour a structural model for directional reversal, and we suggest one possible such model in which the strong binding (force-holding) states of these two motors are essentially

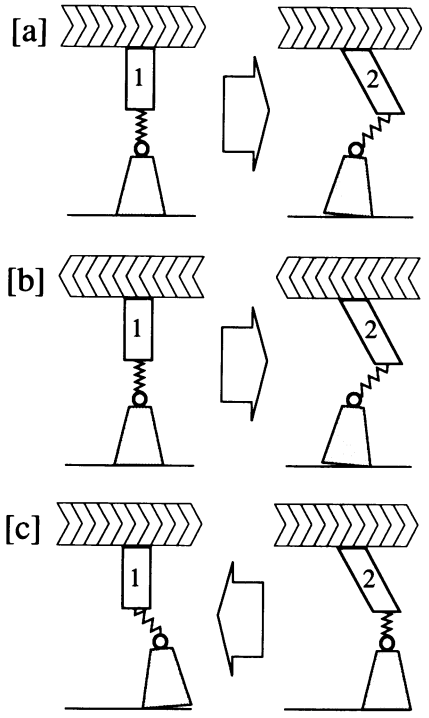

Fig. 1. Possible mechanisms for directional reversal of a molecular motor. (**a**) is a conventional power stroke. The motor drives from state 1 to state 2, exerting force. In (**b**) the motor still drives from state 1 to state 2 but force is produced in the opposite direction because of a 180° rotation within the motor–track complex (shown here at the track–motor interface). In (**c**), the orientations of motor and track, and the structures of states 1 and 2 are all the same as in (a), but the coupling to ATP turnover (represented by the arrow) is altered, such that the motor drives from state 2 to state 1, producing reverse-directed force.

identical, but the weak binding states are biased in mutually opposite directions.

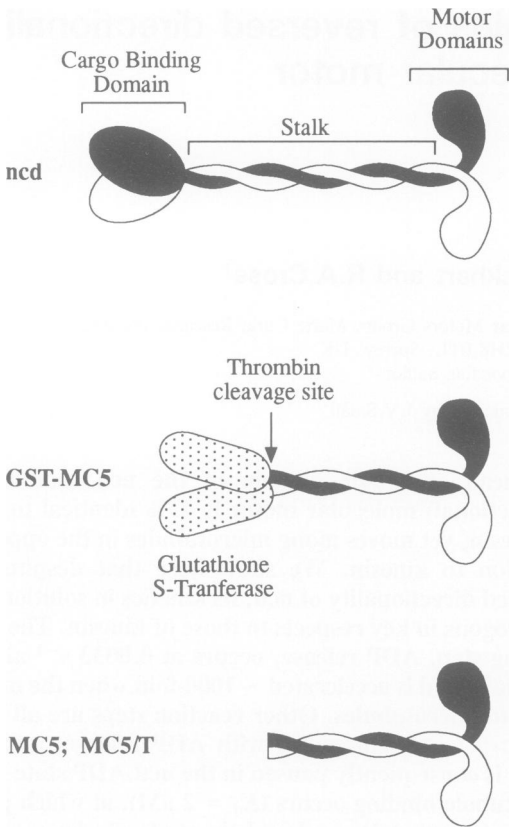

Fig. 2. Schematic representation of ncd and GST–MC5. The wild type protein contains twin C-terminal motors and an N-terminal cargo binding domain separated by a stalk region of predicted coiled-coil. The motor domain contains microtubule binding sites and the ATPase activity of the protein. GST–MC5 was formed by the fusion of MC5, a deletion mutant (residues 294–700) containing all of the motor domain and part of the coiled-coil region of the C-terminus of GST (Chandra *et al.*, 1993). MC5/T is the product of limited thrombin digestion of GST–MC5, and is two residues longer than MC5.

Results

Recombinant GST–MC5 fusion protein

The full-length ncd clone is largely insoluble when expressed in *Escherichia coli*, making the recovery of workable quantities of the protein difficult. Removal of the putative cargo-binding domain of ncd by deletion mutagenesis increases the yield of soluble, active protein. Fusion of this truncated molecule (MC5; Figure 2) to glutathione *S*-transferase (GST) further increases the yield. This fusion protein, GST–MC5, drives microtubule sliding in *in vitro* motility assays with near wild type velocity and displays a microtubule stimulated ATPase activity (Chandra *et al.*, 1993). Unfused MC5 does not drive *in vitro* motility of microtubules (Chandra *et al.*, 1993). For this reason, and because of the increased yields, we have used GST–MC5 routinely in the experiments described here. The rates of the rate-limiting steps of both MC5 and GST–MC5 are indistinguishable over the range 0–800 mM NaCl (see next section), despite the fact that MC5 exists as a dimer in solution, whilst GST–MC5 is reported to be a mix of dimers and tetramers (Chandra *et al.*, 1993).

ADP release is the rate-limiting step of the ncd ATPase

As the binding of ATP to GST–MC5 does not detectably increase the intrinsic fluorescence of the protein, we followed the turnover of ATP using a fluorescent ATP analogue, methylanthraniloyl-ATP (mantATP). This compound has previously been used to investigate the kinetics of kinesin (Sadhu and Taylor, 1993). Figure 3 shows the reaction of GST–MC5 with mantATP. The rising phase of the trace represents the enhancement of mantATP fluorescence on binding to the active site of the protein. On completion of binding we added a 100-fold molar excess of ATP to compete out further binding of mant nucleotides and then recorded the decay in fluorescence, representing the loss of mantADP from the protein. mantADP was released with single exponential kinetics at a rate of 0.0033 s^{-1} at 100 mM NaCl. This value varied linearly over a range of NaCl concentrations from 0 to 400 mM (Figure 4). In all cases the fluorescence decay records were well-fitted by single exponentials (Figure 3), indicating that our GST–MC5 preparation is kinetically homogeneous. This contrasts notably with the behaviour of conventionally purified kinesin, when multiple enzyme populations are observed in transient kinetic assays, owing to the kinesin heavy chain carrying a variable complement of light chains (Hackney, 1988, 1991, 1992). The use of recombinant protein is helpful in simplifying and defining the system (Gilbert and Johnson, 1993).

The initial, rising phase of the records could also be fitted to a single exponential, and these rates were similar to, but

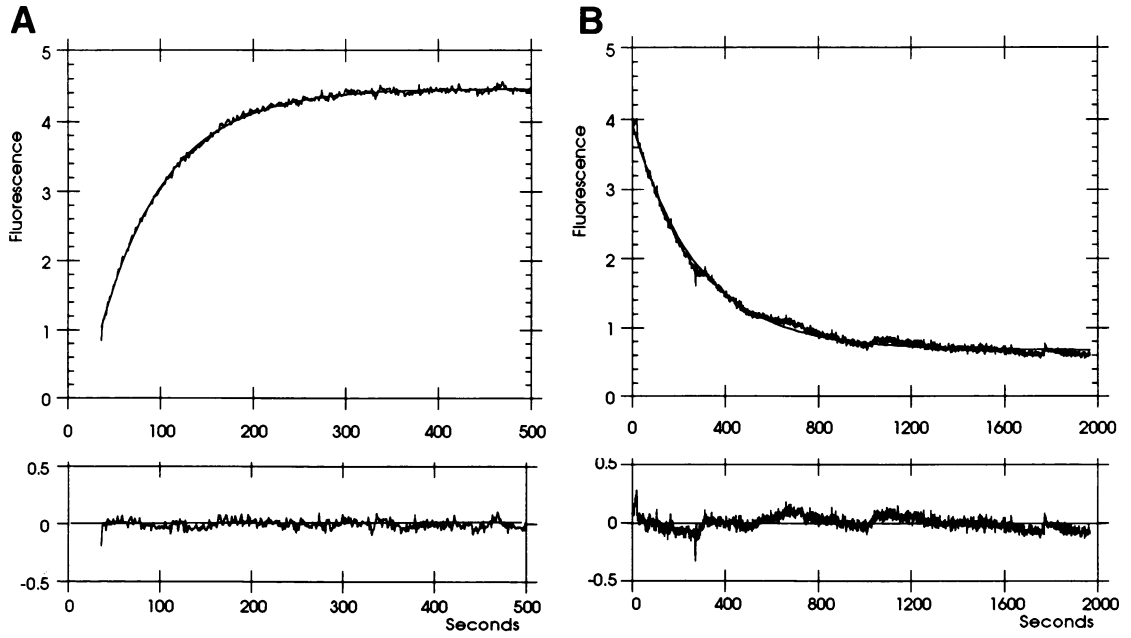

Fig. 3. Time course showing the turnover of 5 μM mantATP by 5 μM GST−MC5 in 100 mM NaCl. After completion of the binding reaction (left panel), the reaction was quenched by addition of a 100-fold molar excess of ATP, and recording of the decay phase (right panel) begun. The data were fitted to single exponentials, represented by the smooth lines, using KFIT. The lower panels show the residuals to the fits.

not identical to, the rates of mantADP release (Figures 3 and 4). The rate of mantATP binding was unaffected by a 10-fold increase in mantATP concentration. On the basis of this finding, and by analogy with the kinesin case (Hackney, 1988) we hypothesized that ADP was already bound to the GST−MC5 used in the experiments.

Further weight was lent to this idea by directly measuring the rate of ADP release from the protein using ATP radiolabelled on its adenine ring (data not shown: see Materials and methods). The rate constant for ADP release calculated in this manner (0.0043 s^{-1} at 100 mM NaCl) was similar to the rate constant for the binding of mantATP in the single turnover assays (Figure 4).

Furthermore, the rate of mantATP binding showed a parallel dependence on ionic strength to the rate of mantADP loss. It thus seemed that GST−MC5 as isolated already contains ADP in its active sites, and that the binding of mantATP is slow because of the requirement that this ADP first dissociate. Since the rate of mantATP binding is limited by the rate of ADP loss, we infer that the rising phase of turnovers such as that in Figure 3 indeed reports the rate of ADP loss from the protein. The rates of ADP loss determined in this way were similar to, but not identical to, the measured rates of mantADP loss. The difference between the two was greatest at very low ionic strength (Figure 4).

In order to check the proportion of active enzyme in our GST−MC5 preparation, we compared the steady state rate of ATP turnover, measured using a linked assay (see Materials and methods), with the measured rate of mantADP binding. The two were identical within experimental error (Figure 4), indicating that contamination of our GST−MC5 preparation with inactive or aberrantly active enzyme is negligibly low. The single turnover methods employed here have the twin advantages of sensitive detection of minority populations, coupled with the ability to measure the rate constant of the major population in the presence of contaminating minor populations.

We have attempted to generate a stable nucleotide-free

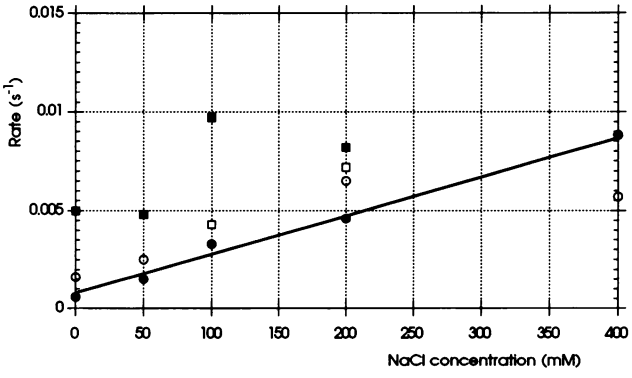

Fig. 4. Dependence of mantADP and ADP release on NaCl concentration. The filled circles are the rate constants determined for mantADP release from GST−MC5, obtained by fitting single exponentials to fluorescence decay records as shown in Figure 3. The open circles are analogous determinations made using MC5 alone and show that the GST moiety has negligible effect on the measured rate constants over a range of NaCl concentrations. The filled squares are the rates of mantATP binding determined under the same conditions, which we argue report the rates of ADP release from GST−MC5. The open square at 100 mM NaCl represents a direct measurement of the rate of ADP release by rapid FPLC gel filtration (see Materials and methods). The open square at 200 mM NaCl is the rate of ATP turnover under these conditions determined in a linked assay system (described below).

form of GST−MC5, in order to measure the rate of mantATP binding to nucleotide-free ncd. Treatment of isolated GST−MC5 with EDTA or apyrase (which hydrolyses ADP and ATP), followed by gel filtration led in our hands to inactivation of the protein, except in the presence of microtubules (see next section). The ncd motor domain thus appears to need either bound nucleotide or microtubules for stability under all the conditions we have tried to date. This has hindered our attempts to look at the faster steps in the reaction pathway, namely ATP binding, ATP hydrolysis and P_i release. However, using rapid gel filtration experiments with γ-^{32}P labelled ATP, we found

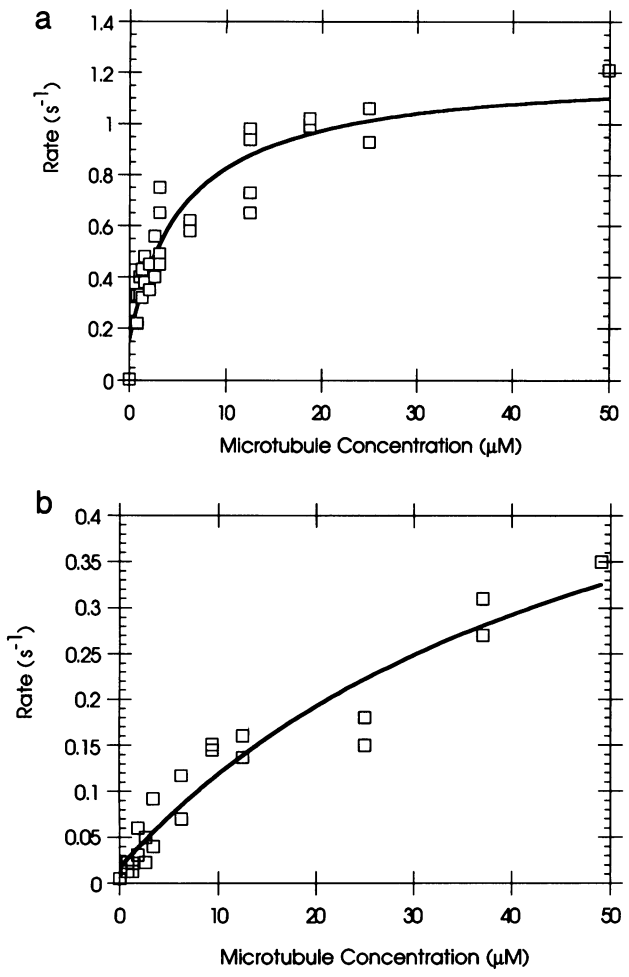

Fig. 5. Steady state measurement of the microtubule activation of the GST−MC5 ATPase at 0 mM NaCl (**a**) and 100 mM NaCl (**b**). The activation curves shown were fitted to rectangular hyperbolae using KFIT to derive the values of V_{max} and the concentrations of tubulin required for half-maximal activation. V_{max} at 0 mM NaCl was 1.05 s^{-1}, and at 100 mM NaCl 0.64 s^{-1}. The concentrations of tubulin required for half-maximal activation were 5.74 μM at 0 mM NaCl and 54 μM at 100 mM NaCl.

that all the P_i was cleaved and released within the dead-time of the technique (1 min). This places a lower limit on the combined rate of nucleotide hydrolysis and P_i release of ~0.1 s^{-1}.

Microtubule binding activates ADP release

Efficient (tight) coupling between ATP turnover and force production by molecular motors depends on acceleration of the rate limiting step by the binding of the motor to its track. Consistent with tight coupling, we find that microtubules accelerate the V_{max} for ADP release from GST−MC5 by three orders of magnitude to 1.05 s^{-1} at 0 mM NaCl (Figure 5). At 100 mM NaCl V_{max} for GST−MC5 is 0.64 s^{-1}, and is thus essentially independent of ionic strength (Figure 5). By contrast, the amount of microtubules required for activation was heavily ionic strength dependent, half-maximal activation requiring 5.74 μM tubulin at 0 mM NaCl and 54 μM tubulin at 100 mM NaCl. The lack of data points at saturating tubulin concentrations in the 100 mM NaCl data set may mean that the values for V_{max} and the amount of tubulin required for half-maximal activation are underestimated. Thus at low ionic strengths, corresponding

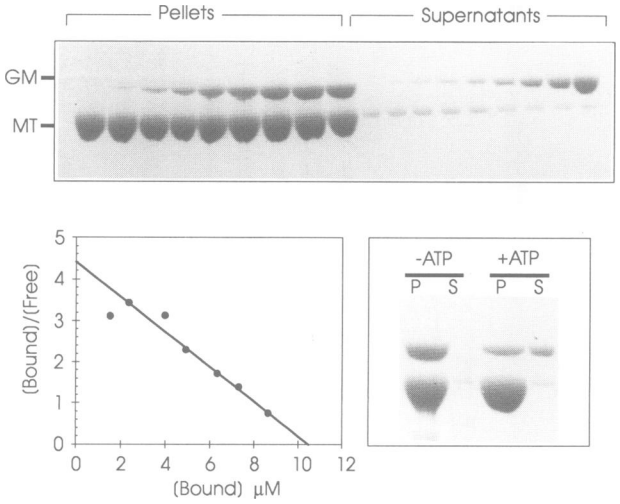

Fig. 6. Sedimentation of GST−MC5 with microtubules. The upper panel shows equivalent loadings of the pellet and supernatant fractions obtained over a range of between 1 and 20 μM GST−MC5, at 10 μM microtubules (labelled GM and MT, respectively). The Scatchard plot at lower left yields an estimate of K_d of 2 μM. The lower right panel shows the effect of apyrase on the binding of GST−MC5 to the microtubules. In the presence of apyrase, which sequesters and hydrolyses free ATP and ADP, GST−MC5 is depleted of nucleotide and pellets essentially quantitatively with the microtubules. Addition of 10 mM ATP to this rigor complex causes partial release of GST−MC5, in line with the measured K_d, and demonstrates that the apyrase treatment has not denatured the protein.

to those commonly used in motility assays, microtubule activation of the rate-limiting ADP release step is more efficient, suggesting that the GST−MC5.ADP complex binds more tightly to microtubules under these conditions.

Do other steps on the reaction pathway also sense microtubule binding? At subsaturating levels of microtubules, we found the rates of mantADP release, measured in single turnovers, correspond to the overall ATPase cycle rate, measured using steady state linked assays. At low microtubule concentrations therefore, ADP release does still appear to be the rate-limiting step of the cycle. Nonetheless, we cannot exclude at this stage that at, or close to, saturating microtubule concentrations, another step on the pathway becomes rate-limiting, and that the rate of this step might respond to microtubule binding. Investigation of this question will require technical improvements to permit work at higher time resolution and with relatively viscous microtubule solutions.

Nucleotide-free ncd binds tightly to microtubules

The interaction of GST−MC5 with microtubules in solution can be followed quantitatively using microtubule pelleting assays. Incubation of GST−MC5 with microtubules in the absence of added nucleotide results in significant binding to the microtubules (Figure 6, upper panel). Using densitometry to determine the distribution of GST−MC5 between the supernatant and pellet, we estimate the K_d of GST−MC5.ADP for microtubules to be 2 μM (Figure 6, lower left panel). Addition of a modest excess (10 μM) of either ADP or ATP has no detectable effect on this result (data not shown), reflecting the fact that ncd.ADP is the dominant species in both the presence and absence of added ATP. Addition of larger amounts of ATP (10 mM) does release some of the bound GST−MC5, consistent with the findings of Chandra *et al.* (1993). The addition to

GST−MC5 of apyrase (an enzyme that sequesters and hydrolyses ATP and ADP), results in the formation of nucleotide depleted GST−MC5, which pellets essentially quantitatively with the microtubules (Figure 6, lower right panel). Nucleotide depleted GST−MC5 appears to be stabilized by its binding to microtubules, since it is released from this rigor-like complex on addition of further ATP (Figure 6, lower right panel). This is consistent with the regeneration by ATP binding of the relatively weakly attached GST−MC5.ADP state, and demonstrates that the increased binding on treatment with apyrase is not due to protein denaturation. Lastly, as a control on the possible influence of the GST moiety on the binding of GST−MC5 to microtubules, we performed a binding experiment in which the GST domain of the fusion protein was cleaved away using the single thrombin site in the linkage between it and the MC5 domain. The resulting species, MC5/T, was fully enzymically active and bound microtubules with the same affinity as GST−MC5 (data not shown).

Discussion

Reaction pathway and kinetic coupling

Using purified bacterially expressed recombinant protein, we have analysed the kinetic cycle of the ncd ATPase. The data are consistent with the minimal kinetic scheme shown in Figure 7, in which the ATP binding step, the hydrolysis step and the P_i release step are all rapid compared with ADP release. The cycle of ATP turnover is effectively paused at the ncd.ADP complex until microtubule binding occurs, triggering ADP release and generating a strongly bound (rigor-like) conformational state of ncd. The key finding of this work is thus that microtubule dependent ADP release switches ncd from a weak binding to a strong binding conformational state.

Comparison with kinesin

The above results identify remarkable kinetic similarities between ncd and kinesin. For kinesin, ADP release is rate-limiting at $\sim 0.003\ s^{-1}$, and is specifically accelerated by microtubules to a V_{max} of $\sim 3\ s^{-1}$, for both ATP (Hackney, 1988) and mantATP (Sadhu and Taylor, 1993). Reported values differ slightly because of heterogeneity in the kinesin preparations. Hackney (1991) has shown that part of this heterogeneity is due to variable content of kinesin beta chains (also called light chains), which appear to facilitate folding up of the molecule with accompanying trapping of bound nucleotide. The use of recombinant kinesin heavy chain (McDonald *et al.*, 1990; Gilbert and Johnson, 1993) eliminates ambiguities due to light chain content. Using transient methods, Sadhu and Taylor (1993) determined rate constants for mantATP binding ($170\ s^{-1}$) and mantATP hydrolysis ($6-7\ s^{-1}$). Phosphate release was shown to be faster than $0.1\ s^{-1}$. All of these data are consistent with what we find for ncd. Different published values for the microtubule concentration for half-maximal activation of the kinesin ATPase may mean that this number is sensitive to salt concentration, as we find for ncd. We conclude that the kinetics of the rate-limiting ADP release step of ncd are essentially identical to those of kinesin.

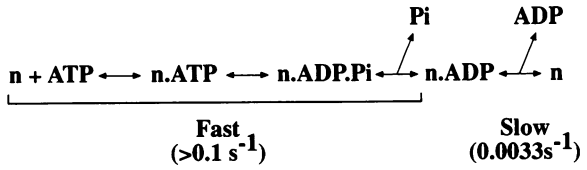

Fig. 7. Scheme for the hydrolysis of ATP by ncd in the absence of microtubules. The combined rate of ATP binding, hydrolysis and phosphate release is at least 30-fold faster than ADP release.

The power stroke and the determinants of directionality

We have shown here that for ncd, as for kinesin, tight coupling between ATP turnover and force generation occurs because rate-limiting ADP release is dramatically accelerated by microtubule binding, triggering the motor to lock onto the microtubule. In a persuasive two-state model for myosin, the switch from weak to strong binding of the track directly produces force (Geeves, 1989). This might be true also of kinesin and/or ncd, but importantly, it need not necessarily be. Romberg and Vale (1993) presented a model for the kinesin mechanism in which ADP release indeed locks the motor to the track, but force is produced by subsequent transition to a strongly bound .ATP or .ADP.P_i state. We have shown here a functional homology between ncd and kinesin at the point of entry into strong binding, the coupled step at which microtubule activated ADP release occurs. The formal possibility remains that, despite the kinetic homology of their .ADP states, the subsequent states .ATP and .ADP.P_i are kinetically very different between kinesin and ncd. It is possible to imagine a scheme in which for one motor, but not the other, the states .ATP and/or .ADP.P_i are force-generating. This could be enough to induce a kinetic reversal of directionality. Our data thus definitively rule out backwards coupling only in the simplest case of kinesin and ncd both being two-state motors (Figure 1), in which the coupled step, the transition from weak to strong binding, itself produces force. The possibility remains of a kinetic mechanism of reversal based on kinetic differences between the .ATP and .ADP.P_i complexes of kinesin and ncd.

A model mechanism for directional reversal

Despite this uncertainty, however, the data show that for these two oppositely directed motors the kinetics of entry into strong binding are very similar indeed. On this basis, and on the assumption of a two-state motor, we want to suggest a simple model mechanism for directional reversal (Figure 8). In the model, the strong binding states of kinesin and ncd are functionally identical, consequently having the same V_{max} and the same efficiency of microtubule-activated ADP release. Force originates directly in the switch from weak to strong binding, and the two motors are postulated to differ only in their initial, weak binding, which is biased in one direction for ncd, and in the other for kinesin. The result of this is that switching into the strong state pulls ncd in one direction, and kinesin in the other. The construction of kinesin−ncd hybrid motors using protein engineering, together with careful analysis of transient kinetics and motility, should allow this and other models for directional reversal to be tested definitively.

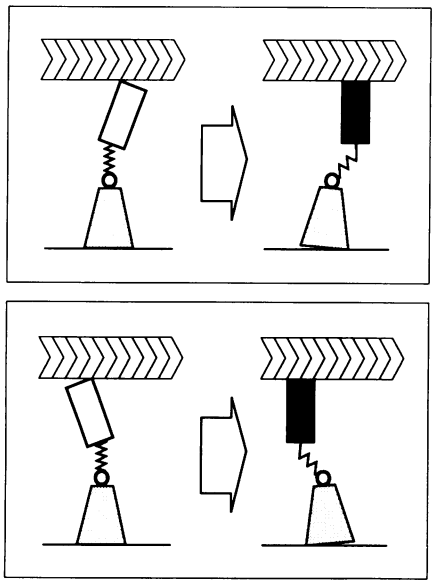

Fig. 8. Model mechanism for the reversal of directionality. The model has two states, a weakly attached (white) state which cannot hold force, and a strongly attached (black) state which can hold force. Transition from the weak to the strong states is coupled in both cases to ADP release. On the basis of the current results, the strong binding states of ncd and kinesin are postulated to be functionally identical, retaining their stereospecificity and their kinetic constants. The two motors differ however in their initial, weak attachment of the white state to the microtubule, which is biased in opposite directions so that subsequent entry into the black state generates oppositely-directed force.

Materials and methods

Expression and purification of GST–MC5

Overnight cultures of BL21 cells harbouring the GST–MC5 vector were diluted 1:50 into 2 × TY medium supplemented with ampicillin (50 μg/ml) and shaken at 37°C for 2 h followed by a further 30 min shaking at 22°C. Expression of GST–MC5 was induced by the addition of isopropyl β-D-thiogalactopyranoside to a final concentration of 0.4 mM. The cells were shaken for a further 4 h at 22°C, harvested by centrifugation, flash frozen in liquid nitrogen and stored at −80°C. The frozen cell pellets were suspended in buffer A (PBS supplemented with 1 mM DTT, 2 mM $MgCl_2$, 1 mM EDTA, 0.5% Triton X-100 and 1 mM PMSF) and incubated on ice with lysozyme (0.1 mg/ml) for 20 min. The cell lysate was made 10 mM $MgCl_2$, 40 μg/ml deoxyribonuclease 1 (Sigma) and incubated for a further 20 min on ice. The lysate was clarified by centrifugation (27 000 *g*, 40 min, 4°C) and the cell pellet discarded.

The supernatant was immediately loaded onto a column packed with glutathione Sepharose 4B (Pharmacia) and equilibrated in buffer A. After extensive washing of the column with buffer A, GST–MC5 was eluted using 50 mM Tris pH 8.0, 1 mM DTT, 2 mM $MgCl_2$ and 20 mM glutathione. Fractions were rapidly analysed by SDS–PAGE (Laemmli 1970) and those containing GST–MC5 were pooled and applied to a Mono S column (Pharmacia) equilibrated with buffer B (20 mM phosphate pH 7.4, 1 mM DTT and 2 mM $MgCl_2$) and step-eluted using buffer A supplemented with 200 mM NaCl as a final purification step. The peak fractions were desalted using an FPLC rapid desalting column (Pharmacia) equilibrated in 20 mM PIPES pH 6.9, 1 mM DTT, 2 mM $MgCl_2$ and 100 mM NaCl. Purified GST–MC5 was stored in this buffer supplemented with 50% glycerol at −20°C. Protein estimation was performed using the Bio-Rad Protein Assay Kit with γ-globulin as the standard. Protein concentrations are based on a monomeric M_r of 73.66 kDa.

Synthesis and purification of mantATP

mantATP was synthesized as described by Hiratsuka (1983) and purified on a DEAE cellulose column with a linear 0.1–1 M triethylamine (pH 7.5) gradient.

mantATP turnover by GST–MC5

mantATP turnover assays were performed in 500 μl reaction volumes at 25°C in 20 mM PIPES pH 6.9, 1 mM DTT, 2 mM $MgCl_2$ over a range of ionic strengths. mantATP (final concentration 5 μM) was mixed with buffer and GST–MC5 added to a final concentration of 5 μM. The reactions were quenched by the addition of ATP to a final concentration of 500 μM. Traces were recorded using a Baird Atomic SFR100 Spectrofluorimeter (λ_{ex} = 350 nm, λ_{em} = 446 nm) linked to a PC fitted with a DAS-1600 A/D converter (Keithley MetraByte) and running KFIT (a kind gift of Dr N.Millar). The traces were fitted to single exponentials using KFIT.

Purification and polymerization of tubulin

Tubulin was purified from porcine brain by two cycles of polymerization and depolymerization, followed by passage over a cellulose phosphate column to remove any microtubule associated proteins. Fractions containing the purified tubulin were pooled, flash frozen in liquid nitrogen and stored at −80°C.

Tubulin was polymerized for use as follows. Aliquots of tubulin (2.5 mg/ml) in buffer C (100 mM PIPES pH 6.9, 2 mM EGTA, 0.5 mM EDTA, 0.5 mM $MgCl_2$, 4 mM DTT and 0.1% β-mercaptoethanol), were polymerized by the addition of $MgCl_2$ and GTP to final concentrations of 1 mM. The tubulin was incubated at 37°C for 1 h, at which point taxol was added to a final concentration of 20 μM.

Microtubule activation of the GST–MC5 ATPase

Steady state ATPase was measured using a pyruvate kinase/lactate dehydrogenase linked assay system (Trentham *et al.*, 1972). The assays were performed in 500 μl reaction volumes at 25°C in 20 mM PIPES pH 6.9, 1 mM DTT, 2 mM $MgCl_2$, 20 μM taxol at either 0 mM or 100 mM NaCl. Phospho(enol)pyruvate, NADH and ATP were added to final concentrations of 3 mM, 0.2 mM and 1 mM, respectively, followed by 16 U of pyruvate kinase, 21.6 U of lactate dehydrogenase and taxol stabilized microtubules. The absorbance of NADH was monitored at 340 nm using a Shimadzu UV-1201 spectrophotometer connected to a PC. A stable baseline was first recorded and then GST–MC5 added to the reaction mixture. The traces obtained were linear over the time scale of the reactions (typically 240–500 s) and were analysed using KFIT to measure the steady state rates. The activation curves were fitted to rectangular hyperbolae using KFIT to derive the values of V_{max} and the concentrations of tubulin required for half-maximal activation.

Microtubule pelleting assays

Pelleting assays were performed in 50 mM PIPES pH 6.9, 2 mM $MgCl_2$, 0.5 mM EGTA, 0.5 mM DTT. GST–MC5 (1–20 μM) was added to taxol stabilized microtubules (10 μM) and the volume adjusted to 100 μl. The mixture was vortexed briefly and centrifuged at 100 000 *g* for 20 min at 20°C. Pellets were resolubilized in 100 μl of 1 M NaCl and equivalent aliquots of the supernatant and pellet fractions were analysed by SDS–PAGE (Laemmli 1970).

Video images of the Coomasie blue stained gels were grabbed into a Mac microcomputer and densitometered using the Freeware programme *Image 1.42* to determine the relative amounts of proteins in the pellets and supernatants. Control experiments established the linearity of this procedure. In the apyrase experiment, 10 U of apyrase (grade III, Sigma) were post mixed into samples prepared as above (see also legend to Figure 6).

Rapid gel filtration assays

2 ml of 10 mM imadazole pH 7.5, 1 mM DTT, 1 mM EDTA, 2 mM $MgCl_2$ and 100 mM NaCl (buffer C) containing 20 μM GST–MC5 and 80 μM of [8-^{14}C]ATP (NEN Research Product, 57 mCi/mmol) were incubated for 5 min at 25°C. The reaction was then quenched with a 100-fold excess of unlabelled ATP. At various time points 200 μl aliquots of the quenched reaction were injected onto a HR10/10 fast desalting column (Pharmacia) equilibrated in buffer C and running at 4 ml/min. Fractions containing GST–MC5 were analysed by scintillation counting to quantitate the amount of radiolabel retained by the protein. The observed decay in radioactivity with time was fitted to a single exponential using KFIT to give a rate constant for ADP release.

Acknowledgements

We thank Drs Sharyn Endow and Rashmi Chandra (née Joshi) for the gift of the GST–MC5 clone, for other clones, for antibodies and for helpful advice. We would also like to thank Dr Danny McKillop for very helpful discussions throughout this work.

References

Chandra,R., Salmon,E.D., Erickson,H.P., Lockhart,A. and Endow,S.A. (1993) *J. Biol. Chem.*, **268**, 9005–9013.

Endow,S.A. (1991) *Trends Biochem. Sci.*, **16**, 221–224.

Endow,S.A. and Titus,M.A. (1992) *Annu. Rev. Cell Biol.*, **8**, 29–66.

Endow,S.A., Henikoff,S. and Soler-Niedzziela,L. (1990) *Nature*, **345**, 81–83.

Geeves,M.A. (1989) *Biochemistry*, **28**, 5864–5871.

Gilbert,S.P. and Johnson,K.A. (1993) *Biochemistry*, **32**, 4677–4684.

Goldstein,L.S.B. (1991) *Trends Cell Biol.*, **1**, 93–98.

Hackney,D.D. (1988) *Proc. Natl Acad. Sci. USA*, **85**, 6314–6318.

Hackney,D.D. (1991) *Biochem. Biophys. Res. Commun.*, **174**, 810–815.

Hackney,D.D. (1992) In *Nucleoside Triphosphatases in Energy Transduction. A Discussion Meeting of the Royal Society*. Eccleston,J.F. Gutfreund,H., Trentham,D.R. and Webb,M.R. (eds), Portland Press, London.

Hatsumi,M. and Endow,S.A. (1992) *J. Cell Sci.*, **101**, 547–559.

Hiratsuka,T. (1983) *Biochim. Biophys. Acta*, **742**, 496–508.

Laemmli,U.K. (1970) *Nature*, **227**, 680–685.

McDonald,H.B., Stewart,R.J. and Goldstein,L.S.B. (1990) *Cell*, **60**, 991–1000.

Romberg,L. and Vale,R.D. (1993) *Nature*, **361**, 168–170.

Sadhu,A. and Taylor,E.W. (1992) *J. Biol. Chem.*, **267**, 11352–11359.

Scholey,J.M., Heuser,J., Yang,J.T. and Goldstein,L.S. (1989) *Nature*, **338**, 355–357.

Stewart,R.J. Thaler,J.P. and Goldstein,L.S.B. (1993) *Proc. Natl Acad. Sci. USA*, **90**, 5209–5213.

Taylor,E.W. (1993) *Nature*, **361**, 115–116.

Trentham,D.R. *et al.* (1972) *Biochem. J.*, **126**, 635–644.

Vale,R.D. and Goldstein,L.S.B. (1990) *Cell*, **60**, 883–885.

Walker,R.A., Salmon,E.D. and Endow,S.A. (1990) *Nature*, **347**, 780–782.

Received on August 19, 1993; revised on November 23, 1993